Available online at www.sciencedirect.com
SCIENCE DIRECT®
Bioelectrochemistry 61 (2003) 99–107
Bioelectrochemistry
www.elsevier.com/locate/bioelechem

Theoretical analysis of the thermal effects during in vivo tissue electroporation

Rafael V. Davalos[a], Boris Rubinsky[a], Lluis M. Mir[b,*]

[a] *Biomedical Engineering Laboratory, Department of Mechanical Engineering, 6178 Etcheverry Hall-University of California at Berkeley, Berkeley, CA 94720-1740, USA*
[b] *Vectorology and Gene Transfer, UMR 8121 CNRS, Institut Gustave-Roussy, 39 rue Camille Desmoulins, F-94805 Villejuif, Cédex, France*

Received 10 October 2002; received in revised form 12 February 2003; accepted 30 July 2003

Abstract

Tissue electroporation is a technique that facilitates the introduction of molecules into cells by applying a series of short electric pulses to specific areas of the body. These pulses temporarily increase the permeability of the cell membrane to small drugs and macromolecules. The goal of this paper is to provide information on the thermal effects of these electric pulses for consideration when designing electroporation protocols. The parameters investigated include electrode geometry, blood flow, metabolic heat generation, pulse frequency, and heat dissipation through the electrodes. Basic finite-element models were created in order to gain insight and weigh the importance of each parameter. The results suggest that for plate electrodes, the energy from the pulse may be used to adequately estimate the heating in the tissue. However, for needle electrodes, the geometry, i.e. spacing and diameter, and pulse frequency are critical when determining the thermal distribution in the tissue.

Keywords: Bioheat equation; Thermal effects; Joule heating; Electrochemotherapy; Electrogenetherapy; Electropermeabilization

1. Introduction

Tissue electroporation, also termed electropermeabilisation, is becoming an increasingly popular method to introduce small drugs and macromolecules into cells in specific areas of the body. This technique is accomplished by placing electrodes into or around the targeted tissue to generate a pulsed electric field inside the tissue [1]. These fields induce reversible (or irreversible) structural changes in the cell membrane that enhance the penetration of these substances into the cytosol [2]. The two most prevalent applications of in vivo tissue electroporation are gene therapy, electrogenetherapy (EGT) [3], and cancer therapy, electrochemotherapy (ECT) [1,4]. Research on the practice of tissue electroporation focuses primarily on characterizing the electric pulse parameters that maximize the amount of electroporated tissue in the targeted area while minimizing damage to the surrounding tissue [5]. While the amount of tissue electroporated by the electric pulses is the most important effect, there are secondary effects from the electrical currents that need to be considered when designing electroporation protocols. One of the most important secondary effects is that of Joule heating.

Biological cells are sensitive to temperature. The damaging effect of elevated temperatures on biological materials has been investigated for decades [6]. A review of the effects of elevated temperatures on biological materials can be found in Ref. [7]. With respect to electrical trauma consequences, an extensive review on the thermal effects of electrical currents can be found in Ref. [8]. In addition, the thermal effects of electroporation have been addressed in several publications. When the skin is exposed to an electropermeabilizing electric pulse, researchers estimated that the increase in temperature should be on the order of 1–10 °C and considered insignificant. However, due to structural changes that result in the creation of highly localized sites from the electroporation itself, the stratum corneum undergoes substantial localized heating [9]. Gallo et al. [10] found that the threshold for electroporation dropped while the recovery time increased at elevated temperatures for experiments with porcine skin. Recently, Kotnik and

* Corresponding author. Tel.: +33-1-42-11-47-92; fax: +33-1-42-11-52-45.
E-mail address: luismir@igr.fr (L.M. Mir).

1567-5394/$ - see front matter © 2003 Elsevier B.V. All rights reserved.
doi:10.1016/j.bioelechem.2003.07.001

Miklavčič [11] developed a theoretical model to estimate the power dissipation in individual cells during electroporation and postulated that heating considered insignificant at the macroscopic level might actually be substantial to the cell membrane.

The goal of this work is to analytically investigate the effect of various parameters on the resultant temperature distribution throughout tissue exposed to permeabilizing electric pulses. This information can be used to provide guidance when designing electroporation protocols. The nature of this problem is complex and assumptions were made in order to capture the essence of the problem while making it tractable. To this end, we have employed the Laplace equation to calculate the electrical potential distribution in tissue during typical electroporation pulses and a modified Pennes (bioheat) equation to calculate the resulting temperature distribution. It is important to note that there are several forms of the bioheat equation, which have been reviewed in Refs. [12,13]. While the Pennes equation is controversial, it is nevertheless commonly used because it can provide an estimate of the effects of various biological heat transfer parameters, such as blood flow and metabolism. The modified Pennes equation employed in this study contains the Joule heating term in the tissue as an additional heat source.

2. Model

In this study, we examined how the Joule heating associated with an electric pulse thermally affects the tissue relative to other factors such as metabolism, blood perfusion, and the heat exchange between the electrode and the tissue. Even though the method outlined in this paper can be used with any geometrical configuration, two important examples were employed to provide insight as to how these various parameters affect the heating associated with electroporation. The first configuration has the tissue placed between two plate electrodes and the second has two needle electrodes embedded in the tissue. In the needle configuration, the analyzed tissue was arbitrarily chosen to be a 32-mm square. These electrode types were chosen because plate and needle electrodes are commonly used in tissue electroporation [3].

In order to keep the problem tractable and mathematically feasible, many simplifying assumptions were made. The analyzed domains are only of the tissue and the electrodes themselves are interpreted as part of the boundary conditions imposed on the tissue. The boundaries of the analyzed domains that are not in contact with the electrodes were assumed to be electrically and thermally insulating. This provides an upper limit to the problem but presumes that the tissue is not heated outside the analyzed domain. In addition, we assumed that heat exchange may occur through the electrodes, but the electrodes themselves are artificially kept at room temperature in order to mathematically exploit the effect of the applied thermal boundary condition, which is maximized when the temperature differential between the tissue and the electrode is largest. Therefore, tissue damage as a direct result from the electrodes heating was not considered. To keep the problem general, it is further assumed that the tissue is isotropic and macroscopically homogeneous. For applications specific to cancer therapy, the malignant tissue can be modeled as a subset of the surrounding tissue. For applications specific to anisotropic tissues such as skeletal muscle, the analysis should be modeled as such. While the electrical conductivity of tissue may increase as a direct result of the electroporation [14], this term is kept constant because the increase has not been well established. Since the analysis is based on an assumption of homogeneous properties and since the variation of electrical conductivity due to electroporation is within the range of tissue inhomogeneity, keeping the term constant retains the same order of accuracy within the entire analysis.

The problem is modeled as two-dimensional for tractability and, therefore, can be interpreted as an upper limit estimate for the amount of heating generated from an electroporation procedure. For the plate configuration, the tissue and electrodes are modeled as infinitely long, essentially a one-dimensional slab, to provide a more conservative approximation of the heating. The thermal distribution is inherently a three-dimensional problem since the electrode length is not infinite but generally comparable to the electrode spacing. A three-dimensional model should be used if less conservative calculations are desired.

3. Method

The most commonly used equation to solve heat transfer problems in the body is Pennes' (1948) bioheat equation, which accounts for metabolism and blood flow [15]:

$$\nabla \cdot (k \nabla T) + w_b c_b (T_a - T) + q''' = \rho c_p \frac{\partial T}{\partial t} \tag{1}$$

where k is the thermal conductivity of the tissue, T is the temperature, w_b is the blood perfusion, c_b is the heat capacity of the blood, T_a is the arterial temperature, q''' is the metabolic heat generation, ρ is the tissue density, and c_p is the heat capacity of the tissue.

The temperature distribution associated with an electroporation pulse can be calculated by simultaneously solving the bioheat equation with the Laplace equation for potential distribution:

$$\nabla \cdot (\sigma \nabla \phi) = 0 \tag{2}$$

where ϕ is the electrical potential and σ is the electrical conductivity. The electrical boundary condition of the tissue that is in contact with the one of the electrodes is defined as

$$\phi = V_o \tag{3}$$

Table 1
Biophysical properties used in analysis

Quantity	Symbol	Units	Value	Reference
Electrical conductivity	σ	S/m	0.286	[18]
$\Delta\sigma/\sigma/\Delta T$	α	%/C	1.50%	[17]
Tissue thermal conductivity	K	W/m K	0.5	[17]
Tissue heat capacity	c_p	J/kg K	3750	[17]
Tissue density	ρ	kg/m^3	1000	[17]
Blood heat capacity	c_b	J/kg K	3640	[17]
Initial temperature	T_0	°C	37	–
Room temperature	T_s	°C	25	–

where V_o is the applied voltage. The electrical boundary condition at the interface of the other electrode and the tissue is defined as

$$\phi = 0 \tag{4}$$

The boundaries where the analyzed domain is not in contact with an electrode are treated as electrically insulative:

$$\frac{\partial \phi}{\partial n} = 0 \tag{5}$$

Solving the Laplace equation enables one to calculate the associated Joule heating, the heat generation rate per unit volume from an electric field (p):

$$p = \sigma \,|\, \nabla \phi \,|^2 \tag{6}$$

This term is added to Eq. (1) to represent the heat generated from the electroporation procedure:

$$\nabla \cdot (k \nabla T) + w_b c_b (T_a - T) + q''' + p = \rho c_p \frac{\partial T}{\partial t} \tag{7}$$

Since most finite-element codes cannot handle the term associated with blood perfusion in the bioheat equation, a simple variable substitution was applied to overcome this limitation. Let

$$T - T_a = U e^{\frac{-w_b c_b t}{\rho c_p}} \tag{8}$$

The transformation looks as such

$$\begin{aligned}(\nabla \cdot k \nabla U) e^{\frac{-w_b c_b}{\rho c_p} t} - w_b c_b U e^{\frac{-w_b c_b}{\rho c_p} t} + (q''' + p) \\ = \rho c_p \frac{\partial U}{\partial t} e^{\frac{-w_b c_b}{\rho c_p} t} - \rho c_p \frac{w_b c_b}{\rho c_p} U e^{\frac{-w_b c_b}{\rho c_p} t}\end{aligned} \tag{9}$$

After canceling out like-terms and dividing through by the exponential, the equation reduces to

$$(\nabla \cdot k \nabla U) + (q''' + p) e^{\frac{w_b c_b}{\rho c_p} t} = \rho c_p \frac{\partial U}{\partial t} \tag{10}$$

Eq. (10) resembles the general heat conduction equation, which is readily solvable with most finite-element packages, with the term $(q''' + p) e^{(w_b c_b / \rho c_p) t}$ as the heat source. The same variable substitution is applied accordingly to the boundary conditions to solve the problem. The solution, U, is subsequently substituted back to determine the temperature distribution in the analyzed domain.

We employed several thermal boundary conditions typical to various configurations between the electrodes and the tissue to study their heat exchange. For a plate electrode, we assumed a heat transfer coefficient between the electrode and its surroundings. This boundary condition takes the form:

$$q'' = h(T_b - T_s) \tag{11}$$

where q'' is the heat flux per unit area, h is heat transfer coefficient, T_b is the electrode–tissue interface temperature, and T_s is the surrounding media temperature.

For a needle electrode, we assumed that it could serve as a fin to remove heat from the electroporated tissue. As a typical estimate, we considered such electrodes to be infinite fins, thereby providing an upper limit for their ability to cool the electroporated-heated tissue. Therefore, we took the equation for the heat dissipation by a fin [19] to be the boundary condition at the electrode–tissue interface.

$$q' = \sqrt{A \cdot k_f \cdot h/P} \cdot (T_b - T_s) \tag{12}$$

where q' is the heat flux per unit length, P is the perimeter, A is the cross-sectional area, and k_f is the thermal conductivity of the fin.

4. Analysis

The analysis modeled conditions typical for electroporation experiments on rat liver [5,16], but used biological parameters corresponding to the human liver. Tissue thermal properties are taken from Ref. [17] and the electrical properties from Ref. [18] and are listed in Table 1.

The intent of the analysis was to determine conditions (electroporation voltage and duration) for which the maximal temperature in the tissue reaches 50 °C, where does it occur and how do the various parameters and conditions affect the occurrence of this maximal temperature. It is assumed that the entire tissue is initially at the physiological temperature (37 °C):

$$T(x, y, z, 0) = T_0 \tag{13}$$

Although thermal damage is a time-dependent process, described by an Arhenius type equation, there are many

Table 2
General parameters for thermal study

Quantity	Symbol	Units	Value			Reference
Voltage	V	V/cm	50	250	1250	[16,20]
Blood perfusion term	w_b	kg/m^3 s	0	0.5	1	[21]
Metabolic heat	q'''	W/m^3	0	16 900	33 800	[21]
Heat transfer coefficient	h	W/m^2 K	0	50	500	[19]

Table 3
Needle electrode specific parameters

Quantity	Symbol	Units	Values			Reference
Electrode diameter	d	mm	0.3	1	1.5	–
Electrode spacing	L	mm	5	7.5	10	–
Electrode conductivity	k_f	W/m K	15	420	–	[19]

reasons 50 °C is generally chosen as the target temperature. Thermal damage begins at temperatures higher than 42 °C, but only for prolonged exposures. Damage is relatively low until 50–60 °C at which the rate of damage dramatically increases. It should also be noted that at this temperature, the pain moves from severe to unbearable [7]. Since the Laplace and heat transfer equations are linear, the data produced can be extrapolated and considered indicative of the overall thermal behavior.

For each configuration, the surface of one electrode is assumed to have a prescribed voltage with the other electrode set to ground. The modeled voltage-to-distance ratios were 50, 250, and 1250 V/cm, all typical values [16,20]. The effect of the spacing between the electrodes, center-to-center for the needle configuration and edge-to-edge for the plate configuration, was investigated by comparing distances of 5, 7.5 and 10 mm. The electrodes were modeled as stainless steel or silver and, for the needle configuration, either 0.3, 1 or 1.5 mm in diameter. The convection parameter in heat transfer analysis was varied from zero, simulating a completely insulating electrode surface, to 50 W/m^2 K simulating convection in air, to 500 W/m^2 K simulating forced convection in fluids. The blood flow perfusion rate was taken to be zero, 0.5 or 1.0 kg/m^3 s [21]. The metabolic heat was taken to be either zero, 33 800 W/m^3 [21] or, to track the metabolic heat influence, the average. A summary of the varied parameters can be found in Tables 2 and 3.

All calculations were performed using MATLAB's finite-element solver, Femlab v2.2 (The MathWorks, Natick, MA). To ensure mesh quality and validity of solution, the mesh was refined until there was less than a 0.5% difference in solution between refinements. For the plate configuration, there was less than a 2% difference from the exact solution, which was calculated for all configurations that neglected blood flow or convective losses through the electrodes. The plate electrode system contained 863 nodes with 1632 triangles, and the needle electrode configuration contained 2044 nodes with 3900 triangles. Pulse durations were calculated with a resolution of at least 1%. The simulations were conducted on a Compaq Presario computer with 256 MB of RAM.

5. Results and discussion

Fig. 1a–d illustrates typical results and show isopotential and isothermal lines that form with a 1-s long, 50-V pulse applied at the electrodes for the two systems. In these

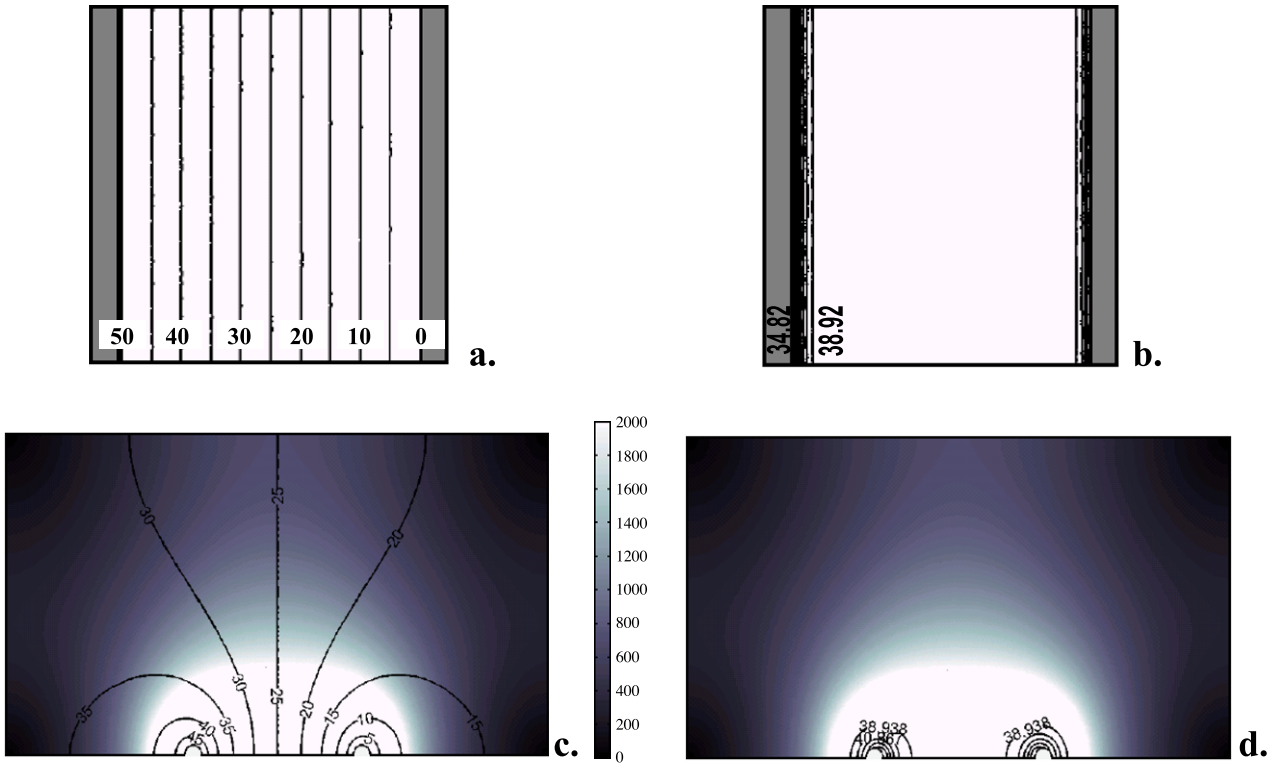

Fig. 1. Analysis of thermal distribution after 1-s 50-V electroporation pulse (q''' = 33 800 W/m^3, h = 500 W/m^2 K, w_b = 0 kg/m^3 s), panel a: isopotential lines, panel b: isothermal lines for plate configuration, panel c: isopotential lines, panel d: isothermal lines with electric field superimposed for needle configuration.

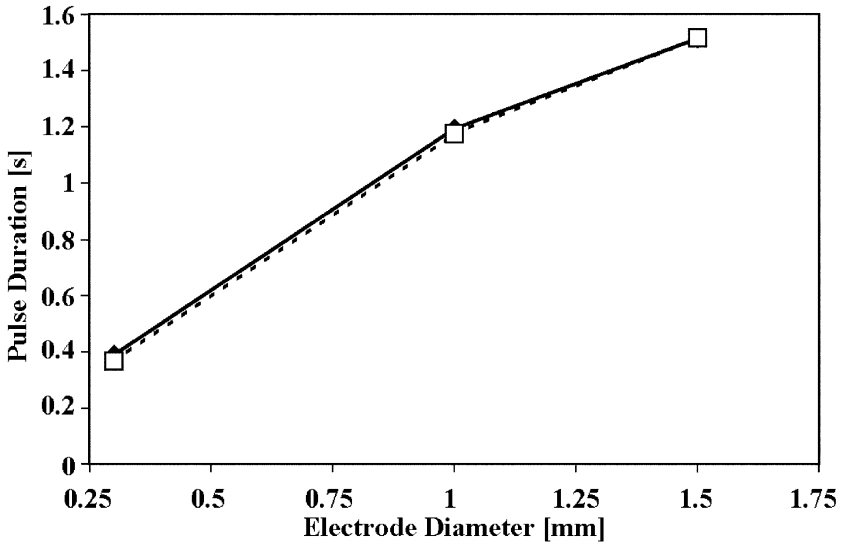

Fig. 2. Effect of electrode diameter on allowable pulse length for tissues with constant and varying ($\alpha = 1.5\%/°C$) electrical conductivity. —◆—, variable conductivity; - □ -, constant conductivity.

particular examples, the electrodes are assumed to be steel with a heat transfer coefficient of 500 W/m^2 K. The distance between the electrodes is 10 mm, with a volumetric blood flow rate of 0 and metabolic heat of 33 800 W/m^3.

With these parameters, the maximum temperature for the plate configuration is located at the center, and the temperature along the electrodes actually drops below the initial 37 °C because of the heat dissipation through the electrodes to the cooler outside environment. However, for the needle electrode configuration, the maximum temperature is always near the electrode surface but rapidly diminishes.

Fig. 2 compares the effect of the electrode diameter for the cylindrical system as well as variations in tissue properties due to temperature. It plots the pulse duration required to achieve a maximum temperature of 50 °C for a 50-V pulse, ignoring blood flow, metabolic heat, and convective losses as a function of electrode diameter for an electrode spacing of 10 mm. The diameters tested are 0.3, 1.0 and 1.5 mm for two different scenarios. The first scenario varies the electrical conductivity as a function of temperature, and the second one maintains a constant conductivity. An electrode diameter and pulse duration combination under these curves will generate a temperature lower than 50 °C while a combination above the curves will generate a higher temperature. For thinner needles, the allowable pulse duration is strongly affected by changes in diameter, but this dependency diminishes as the electrode size increases. These results allow the investigators to adopt the best compromise between thermal or irreversible damage near the electrodes and a larger incision.

If the biological properties are assumed to be constant and the contributions from blood flow, metabolic heat and

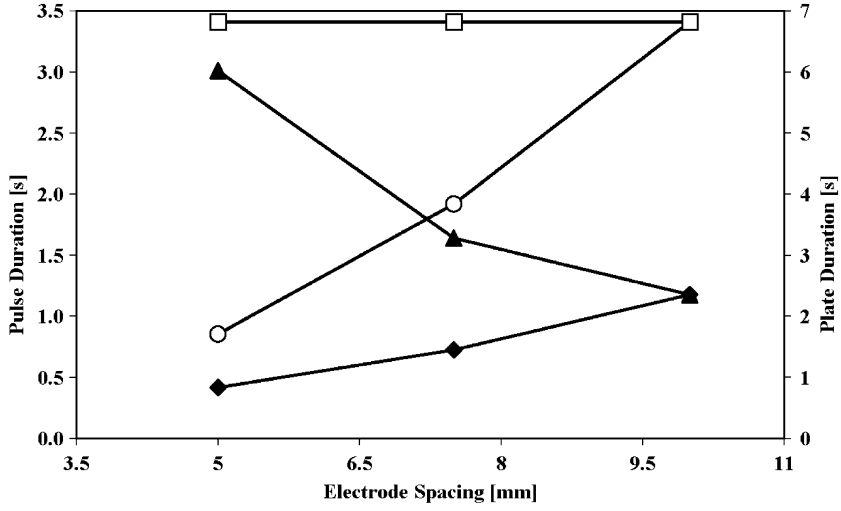

Fig. 3. Effect of electrode spacing on allowable pulse length. —◆—, needle 50/0 V (with one electrode at 50 V and the other grounded); —▲—, needle 50 V/cm; —○—, plate 50/0 V; —□—, plate 50 V/cm.

electrode heat dissipation are neglected; the increase in temperature for the plate configuration is simply calculated from the Joule heating:

$$\Delta T = \frac{\sigma}{\rho c_p} |\nabla \phi|^2 \Delta t \quad (14)$$

However, the thermal and electrical conductivities of biological tissues are both functions of temperature. In liver, for example, they vary 0.25% and 1.5% per °C, respectively [17]. To take into account the tissue properties dependence on temperature, Eq. (14) would need to be solved iteratively. Applying these dependencies to the plate configuration decreases the allowable duration approximately 8% since the tissue properties of the entire domain will change. On the other hand, the results also show that implementing these dependencies only slightly alters the results for the needle configuration. Therefore, in the subsequent calculations, the models are assumed to have constant electrical and thermal conductivities.

Fig. 3 explores the effect of the spacing between the electrodes. It plots the pulse duration required to achieve a maximum temperature of 50 °C for a 50-V pulse, ignoring blood flow, metabolic heat, and convective losses as a function of electrode spacing. From Eq. (14) it should be apparent, as well as expected, that it is not the applied voltage that is important for the plate configuration but rather the total energy generated from a pulse.

For an electrode diameter of 1 mm, the needle electrode configuration was analyzed by first only varying the center-to-center spacing and then by adjusting the voltage along with the spacing such that the voltage-to-distance ratio remained constant. Fig. 3 shows that the allowable duration for the needle configuration actually depends on the voltage-to-distance ratio as well as on the spacing. The allowable pulse lengths for these configurations with an electrode spacing of 10 mm (i.e. 6.818 s for the plate configuration and 1.175 s for the needle configuration) are used as the baseline values for the subsequent calculations in Fig. 4.

Fig. 4a explores the effect of the volumetric blood flow on the temperature distribution in the tissue. This distribution is compared using an electrode spacing of 10 mm, with a pulse voltage and duration that yields a maximal temperature of 50 °C under the conditions discussed in Fig. 3, for three different blood flows. The contributions from blood flow are more noticeable for the plate electrodes because of the longer allowable pulse length. However, in both situations, the contribution is small and may be considered actually less significant because recent studies have shown that soon after the electrical pulses are delivered, the blood flow is restricted in the treated region for up to 2 min [22].

Fig. 4b explores the effect of the metabolic heat on the temperature distribution in the tissue. For an electrode spacing of 10 mm, it shows the pulse duration required for a 50-V pulse to yield a maximal temperature of 50 °C under the conditions discussed in Fig. 3 for a metabolic heat of 33 800 W/m^3 [21], half that value, and without metabolic heat. The conclusion is that the contribution from metabolic heat is virtually nonexistent.

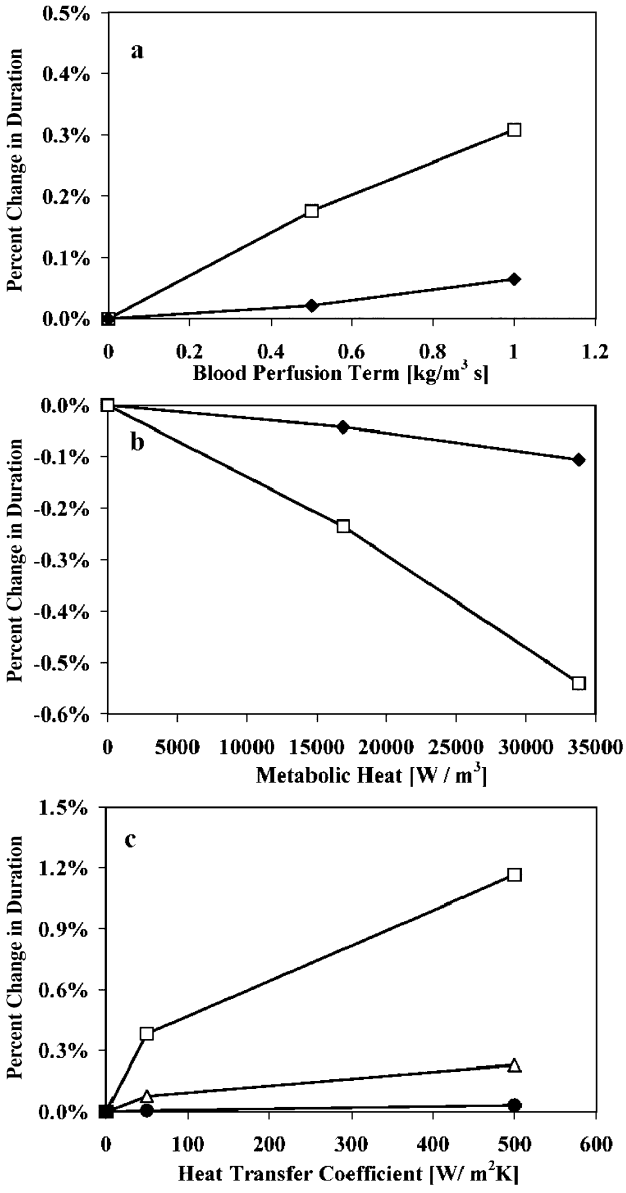

Fig. 4. The effects of (a) blood flow, (b) metabolic heat, and (c) electrode heat dissipation on allowable pulse lengths for baseline values of 1.175 s for the needle configuration and 6.818 s for the plate configuration. Panel a: —◆—, needle configuration; —□—, plate configuration. Panel b: —◆—, needle configuration; —□—, plate configuration. Panel c: —△—, stainless steel, needle; —□—, silver, needle; —●—, plate (steel, silver).

Fig. 4c explores the effect of heat dissipation through the electrodes on the temperature distribution in the tissue. For an electrode spacing of 10 mm, it compares the pulse duration required for a 50-V pulse to yield a maximal temperature of 50 °C under the conditions discussed in Fig. 3 for the three different heat transfer coefficients. Fig. 4c also investigates the effect of electrode material by

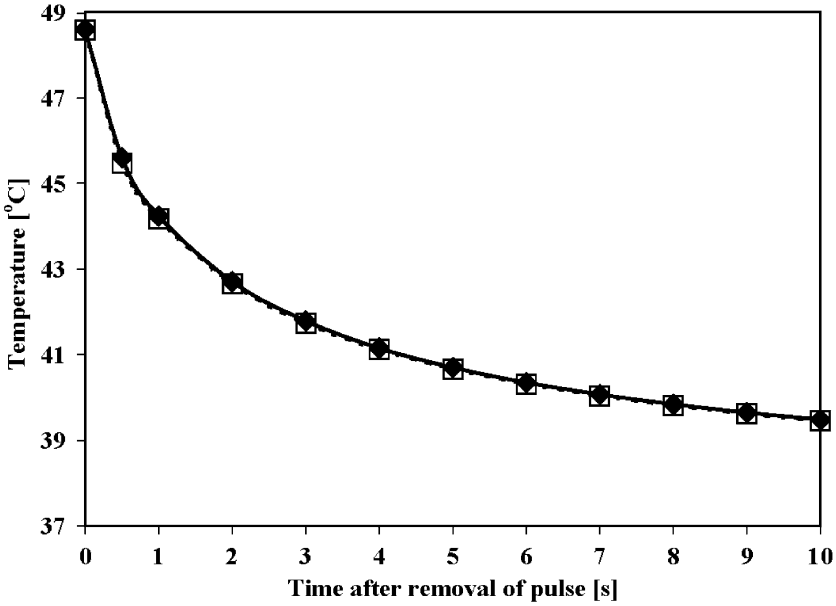

Fig. 5. Heat dissipation after a 1-s 50-V pulse. —◆—, control; - □ -, thermally conductive electrode.

comparing stainless steel and silver electrodes for the cylindrical case in Fig. 3. It was found that during the application of the pulse, the heat dissipation through the electrodes is relatively small.

Because of the short duration of the pulse, Fig. 5 explores the heat dissipation after a 1-s 50-V pulse for the needle configuration with stainless steel electrodes and a heat transfer coefficient of 500 W/m^2 K. The figure suggests two things. The first is that after the removal of the pulse, the temperature rapidly drops, and second is that there is little heat dissipation through the electrodes themselves. It should be pointed out that since these electrodes are assumed to be infinite, they provide an upper limit as to the amount of heat dissipated.

Figs. 6 and 7 compare the required voltage and pulse length to reach 50 °C while neglecting contributions from blood flow, metabolic heat, and heat dissipation through the electrodes for an electrode spacing of 10 mm and, for the needle configuration, an electrode diameter of 1 mm. Typical pulse parameters are usually eight pulses at 1 Hz with 250 V/cm at 50 ms for gene therapy [16] and 1300 V/cm at 100 μs for ECT [1,4,5]. Fig. 6 shows the necessary pulse duration for common voltages (50, 100, 250, 1250 V) to reach 50 °C. Fig. 7 does the opposite and highlights the necessary voltage to reach 50 °C for common pulse lengths (100 μs, 1 ms, 10 ms, 100 ms, and 1 s).

In the case of the plate electrodes, the allowable pulse lengths are much longer than the usual experimental con-

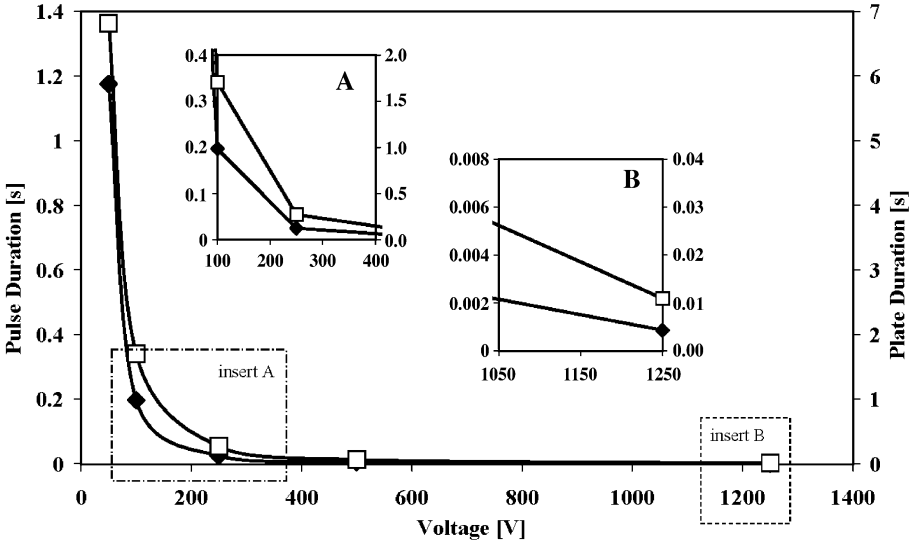

Fig. 6. Voltage vs. pulse duration for maximum temperature of 50 °C. —◆—, needle; —□—, plate.

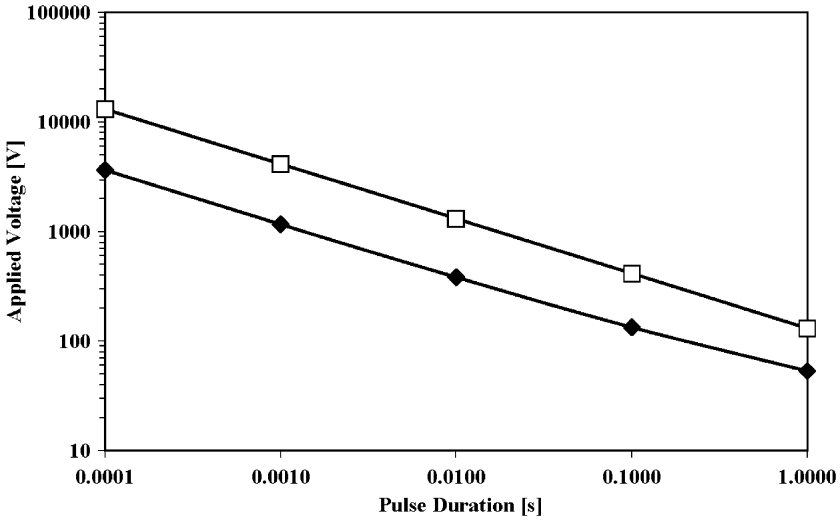

Fig. 7. Pulse duration vs. voltage for maximum temperature of 50 °C. —◆—, needle; —□—, plate.

ditions for ECT and EGT. This implies that if these electrodes are in direct contact with the treated tissue, the heating generated with these electrodes is insignificant. Therefore, if histological alterations are observed, they should be due to the cell electropermeabilization or drug or DNA presence and not to tissue heating. However, since plate electrodes are commonly employed for skin electroporation, the large surface impedance of the skin, the skin-electrode contact resistance, and the creation of highly localized transport regions need to be taken into account [23,24].

In the case of the needle electrodes, the required pulse duration to reach 50 °C is comparable to the total length of the pulses during typical experiments, i.e. eight times a single pulse length. This suggests that the tissue near the electrodes could be irreversibly damaged, which corresponds with results found from Miklavčič [5]. However, these calculations can be considered conservative due to the typical 1-s delay between pulses, which allows for more heat dissipation through the electrodes and blood flow and, most importantly, through the tissue itself. To investigate this effect, Fig. 8 shows, for the needle configuration described in Fig. 3 with an electrode spacing of 10 mm, the difference between one 400-ms 100-V pulse and eight 50-ms 100-V pulses applied at a frequency of 1 Hz. It should be noted that in these calculations, the heating of the electrodes was not considered. The thermal conduction

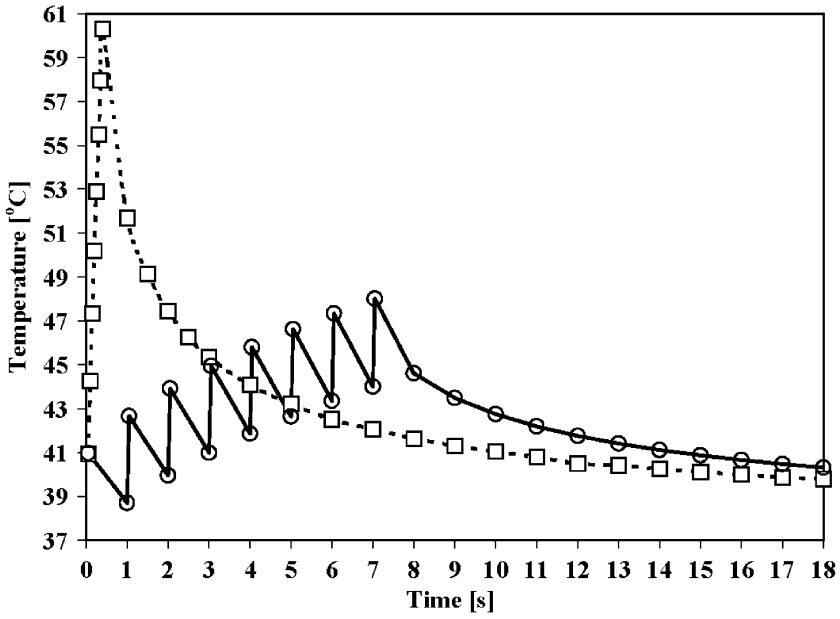

Fig. 8. Comparison between a single pulse and a set of pulses with the same applied duration on the maximal temperature for 100-V pulse(s). - □ -, one 400-ms pulse; —o—, eight 50-ms pulses at 1 Hz.

through the tissue appreciably dissipates the heat in the tissue thereby largely decreasing the maximum temperature experienced by the tissue.

6. Conclusion

In summary, our study shows analytically the effects of various electroporation parameters and conditions on the temperature distribution in tissue during electroporation. As a general rule, the allowable pulse lengths for which there is no part of the tissue exposed to 50 °C are much longer for plate electrodes than for needle electrodes. For the needle electrode configuration, the contributions during a single pulse from blood flow, metabolic heat generation, and electrode heat dissipation were small due to the short allowable duration of the pulse and the concentrated region of the affected tissue. More importantly, for this configuration, it is necessary to look at parameters such as electrode spacing and diameter as well as repetition frequency when designing protocols. For the plate configuration, since the allowable pulse lengths were longer and the entire tissue was affected, the contributions from blood flow, metabolic heat, and electrode heat dissipation were more significant. However, the results suggest that Joule heating alone is a useful estimate of the temperature increase from electroporation for this configuration. In both cases, ignoring the blood perfusion term provides an upper limit estimate for the temperature distribution in the tissue. The contributions from blood perfusion, metabolic heat generation, and electrode heat dissipation were assessed assuming a single pulse, but if multiple pulses were applied, their role would be more significant, and would depend on the pulse repetition frequency. During an electroporation procedure, the amount of heating produced is not negligible. This study should provide the reader with the tools to address the thermal issues associated with electroporation.

Acknowledgements

This research was supported by NIH Grant No. 1 R21 RR15252-01. Rafael Davalos would also like to thank Sandia National Laboratories for their support. L.M. Mir acknowledges the CNRS, the Institut Gustave-Roussy, and the EU commission (Cliniporator QLK3-1999-00484 project) for their general support of his research.

References

[1] L.M. Mir, Therapeutic perspectives of in vivo cell electropermeabilization, Bioelectrochemistry 53 (2001) 1–10.
[2] J.C. Weaver, Electroporation of cells and tissues, IEEE Transactions on Plasma Science 28 (2000) 24–33.
[3] S. Somiari, J. Glasspool-Malone, J.J. Drabick, R.A. Gilbert, R. Heller, M.J. Jaroszeski, R.W. Malone, Theory and in vivo application of electroporative gene delivery, Molecular Therapy 2 (2000) 178–187.
[4] L.M. Mir, L.F. Glass, G. Sersa, J. Teissie, C. Domenge, D. Miklavčič, M.J. Jaroszeski, S. Orlowski, D.S. Reintgen, Z. Rudolf, M. Belehradek, R. Gilbert, M.P. Rols, J. Belehradek, J.M. Bachaud, R. Deconti, B. Stabuc, M. Cemazar, P. Coninx, R. Heller, Effective treatment of cutaneous and subcutaneous malignant tumours by electrochemotherapy, British Journal of Cancer 77 (1998) 2336–2342.
[5] D. Miklavčič, D. Semrov, H. Mekid, L.M. Mir, A validated model of in vivo electric field distribution in tissues for electrochemotherapy and for DNA electrotransfer for gene therapy, Biochimica et Biophysica Acta 1523 (2000) 73–83.
[6] F.C. Henriques, A.R. Moritz, Studies in thermal injuries: the predictability and the significance of thermally induced rate processes leading to irreversible epidermal damage, Archives of Pathology 43 1947, pp. 489–502.
[7] K.R. Diller, in: Y.I. Choi (Ed.), Bioengineering Heat Transfer, Advances in Heat Transfer vol. 32, Academic Press, Boston, 1992, pp. 157–357.
[8] R.C. Lee, D. Zhang, J. Hannig, in: M.L. Yarmish, K.R. Diller, M. Toner (Eds.), Ann. Rev. Biomed. Eng., vol. 2, Annual Review Press, Palo Alto, 2000, pp. 477–509.
[9] U. Pliquett, E.A. Gift, J.C. Weaver, Determination of the electric field and anomalous heating caused by exponential pulses with aluminum electrodes in electroporation experiments, Bioelectrochemistry and Bioenergetics 39 (1996) 39–53.
[10] S.A. Gallo, A. Sen, M.L. Hensen, S.W. Hui, Temperature-dependent electrical and ultrastructural characterizations of porcine skin upon electroporation, Biophysical Journal 82 (2002) 109–119.
[11] T. Kotnik, D. Miklavčič, Theoretical evaluation of the distributed power dissipation in biological cells exposed to electric field, Bioelectromagnetics 21 (2000) 385–394.
[12] C.K. Carney, in: Y.I. Choi (Ed.), Bioengineering Heat Transfer, Advances in Heat Transfer vol. 28, Academic Press, Boston, 1992, pp. 19–122.
[13] T.K. Eto, B. Rubinsky, in: S.A. Berger, W. Goldsmith, E.R. Lewis (Eds.), Introduction to Bioengineering, Oxford Univ. Press, Oxford, 1996.
[14] R.V. Davalos, B. Rubinsky, D.M. Otten, A feasibility study for electrical impedance tomography as a means to monitor tissue electroporation for molecular medicine, IEEE Transactions on Biomedical Engineering 49 (2002) 400–403.
[15] H.H. Pennes, Analysis of tissue and arterial blood temperatures in the resting forearm, Journal of Applied Physiology 1 (1948) 93–122.
[16] T. Suzuki, B. Shin, K. Fujikura, T. Matsuzaki, K. Takata, Direct gene transfer into rat liver cells by in vivo electroporation, FEBS Letters 425 (1998) 436–440.
[17] F.A. Duck, Physical Properties of Tissues: A Comprehensive Reference Book, Academic Press, San Diego, 1990.
[18] K. Boone, D. Barber, B. Brown, Review-imaging with electricity: report of the European concerted action on impedance tomography, Journal of Medical Engineering and Technology 21 (1997) 201–232.
[19] F.P. Incropera, D.P. De Witt, Fundumentals of Heat and Mass Transfer, Wiley, New York, 2002.
[20] L.M. Mir, Therapeutic perspectives of in vivo cell electropermeabilization, Bioelectrochemistry 53 (2001) 1–10.
[21] Z.S. Deng, J. Liu, Blood perfusion-based model for characterizing the temperature fluctuations in living tissue, Physica. A, Statistical Mechanics and its Applications 300 (2001) 521–530.
[22] J. Gehl, T. Skovsgaard, L.M. Mir, Vascular reactions to in vivo electroporation: characterization and consequences for drug and gene delivery, Biochimica et Biophysica Acta 1569 (2002) 51–58.
[23] G.T. Martin, U.F. Pliquett, J.C. Weaver, Theoretical analysis of localized heating in human skin subjected to high voltage pulses, Bioelectrochemistry 57 (2002) 55–64.
[24] U.F. Pliquett, G.T. Martin, J.C. Weaver, Kinetics of the temperature rise with human stratum corneum during electroporation and pulsed high-voltage iontophoresis, Bioelectrochemistry 57 (2002) 65–72.